UNIVERSITÀ DEGLI STUDI DI MESSINA
Scuola di Neuroscienze MED-26
Dottorato di Ricerca in Scienze Biomediche Cliniche e Sperimentali
Ciclo XXIX

In vivo evaluation of carotid artery stenosis: Magnetic Resonance 3.0T vs Ultrasound Imaging

Tesi di Dottorato di:
Dott. Fabrizio SOTTILE

Relatore:
Prof. Giorgio ASCENTI

Anno Accademico 2015/2016

Una vita senza ricerca
non è degna di essere vissuta.
Socrate

Contents

List of Figures

Abstract

Quantitative characterization of carotid atherosclerosis and classification of plaques is crucial in the diagnosis and treatment planning. The degree of carotid stenosis is, up to now, considered one of the most important features for determining the risk of brain stroke. Carotid ultrasonography (US) has been shown to be a useful predictor of incident cardiovascular events. Magnetic resonance (MR) imaging is an alternative approach that can also be used to identify carotid plaque. Carotid MR imaging can accurately depict plaque components, such as the lipid core, and it can be used to identify and monitor vulnerable plaque. The aim of this study was the comparison of segmentation techniques of US images to characterize plaque morphology and composition with the 3T MR, using US image as the gold standard. This analysis was conducted on 22 patients with pathology of the carotid arteries showed an on US examination of Sovraotic Trunch. From each patient, a varying number of images has been taken to form the final dataset. All patients underwent to a MR examination. The US data were obtained as longitudinal cross-sections using a Philips iU22 ultrasound scanner with an L9-3 probe and included B-Mode (i.e. greyscale) and Colour Doppler image sequences. Then all patients underwent to a MR examination on a 3T MR system with Sense Head coil. The same plaque was evaluated by US and MR examination, relatively to size, consistency of plaques, intima-media thickness. Concordance Correlation Coefficient (CCC) was calculated on three extracted parameters to evaluate the consistency of two methods. The subjects presented clinical and vascular risk factors. Two subjects that have hypoechoic plaques not highlighted by MR were excluded. F-test no highlighted significant variance differences between the two methodologies ($p > 0.05$). The values of three plaque parameters obtained by automatic segmentation were highly significantly correlated with those obtained from manual segmentation ($r_1 = 0.78$, $r_2 = 0.84$, $r_3 = 0.89$, with $p < 0.001$). Our results showed a very high comparison between US and MRI examinations. From the results obtained, there were no significant differences between the two techniques. The minimal difference is, probably, related to the fact that the US and MRI numerical data were obtained by the operator in a total manual

modality. However, a limitation of our study is that hypoechoic plaques evaluated with US methodical are difficult to detect by MRI. The obtained results could to argue that MR examination is the most promising objective method.

Chapter 1

Introduction

In this chapter, after a brief description of atherosclerosis, diagnostic techniques will be shown. In addition, we will describe the segmentation techniques to identify a carotid plaque.

1.1 Atherosclerosis

Atherosclerosis is the major cause of carotid artery disease. It can begin in early adulthood, but it usually takes decades to cause symptoms. Some people have rapidly progressing atherosclerosis during their thirties, others during their fifties or sixties. Atherosclerosis begins with damage to the inner wall of the artery caused by high blood pressure, diabetes, smoking, and high cholesterol specifically "bad" cholesterol or low-density lipoprotein (LDL). Other risk factors include obesity, coronary artery disease, a family history of carotid stenosis, and advanced age. Less commonly, carotid aneurysm and fibromuscular dysplasia can cause carotid stenosis. People who have heart disease have an increased risk of developing carotid stenosis. Typically, the carotid arteries become diseased a few

years later than the coronary arteries. Carotid stenosis is a progressive narrowing of the carotid arteries in a process called atherosclerosis. Normal healthy arteries are flexible and have smooth inner walls. As we age, hypertension and small injuries to the blood vessel wall can allow plaque to build up. Plaque is a sticky substance made of fat, cholesterol, calcium, and other fibrous material. Over time, plaque deposits inside the inner wall of the artery can form a large mass that narrows the lumen, the inside diameter of the artery. Atherosclerosis also causes arteries to become rigid, a process often referred to as "hardening of the arteries".

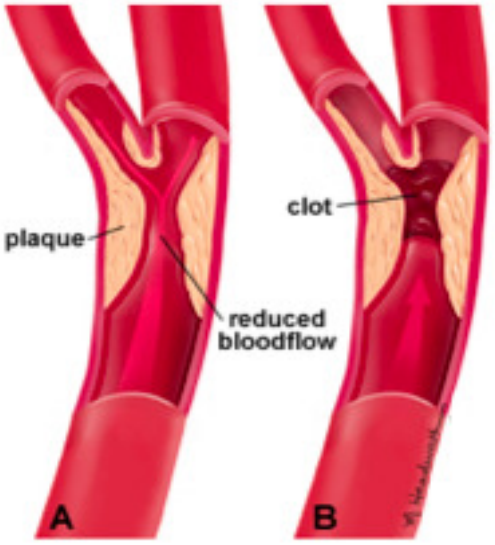

FIGURE 1.1: *A. Atherosclerotic plaque narrows the artery diameter, reducing blood flow. B. The irregular surface of the artery wall can cause clot formation that blocks the vessel or breaks off, travels downstream, and blocks a smaller vessel.*

There are three ways in which carotid stenosis increases the risk of stroke:

- Plaque deposits can grow larger and larger, severely narrowing the artery and reducing blood flow to the brain. Plaque can eventually completely block (occlude) the artery (fig. 1.1A);

- Plaque deposits can roughen and deform the artery wall, causing blood clots to form and blocking blood flow to the brain (fig. 1.1B);
- Plaque deposits can rupture and break away, traveling downstream to lodge in a smaller artery and block blood flow to the brain.

Most people with carotid stenosis have no symptoms until the artery becomes severely narrowed or a clot forms. Symptoms are most likely to first appear with a mini-stroke, also known as a transient ischemic attack (TIA). TIAs result when blood flow to the brain is temporarily interrupted and then restored. The symptoms typically last a couple of minutes and then resolve completely, and the person returns to normal. TIAs should not be ignored; they are a warning that an ischemic stroke and permanent brain injury may be looming. Symptoms of a TIA or an ischemic stroke can include weakness or numbness in an arm or leg, difficulty speaking, a drooping face, vision problems, or paralysis affecting one side of the body. Older people are more likely to be affected by carotid stenosis. Before age 75, men are more at risk than women. A person who has high cholesterol, has high blood pressure, and smokes is eight times more likely to develop atherosclerosis than a person without these risk factors. More than 500,000 new strokes occur in the United States each year, and carotid stenosis is estimated to cause 20 to 30% of them.

1.2 Diagnostic Tecniques

Diagnostic techniques to detect a carotid plaque are:

- Doppler ultrasound is a noninvasive test that uses reflected sound waves to evaluate blood flow through a vessel. The ultrasound probe is placed on

the neck over the carotid arteries. This test will reveal how much blood is flowing through the artery and to what degree the artery has narrowed (i.e., 100%, 80%, 70%, etc.).

- Computed Tomography Angiography is a noninvasive X-ray that provides detailed images of anatomical structures within the brain. It involves injecting a contrast agent into the blood stream so that arteries of the brain can be seen. This type of test provides the best pictures of both blood vessels (through angiography) and soft tissues (through CT). It enables doctors to see the narrowed artery and to determine how much it has narrowed.

- Magnetic Resonance Angiography (MRA) of the neck is similar to the CT angiogram. Contrast dye is injected through an IV to illuminate blood vessels in the neck.

- Cerebral Angiogramis a minimally invasive test that uses X-rays and a contrast agent injected into the arteries through a catheter in the groin. This technique allows to visualize all arteries in the brain.

1.3 Segmentation Tecnique

Segmentation of ultrasound images is essential for quantitative measurement of plaques, by using markers such as shape, area, eccentricity and thickness [1]. Plaque-image segmentation methods allow to isolate the region of diagnostic interest. Noise from the extracted plaques can be removed by using the image despeckling methods. Texture features are subsequently computed over the segmented images. Texture features are then used as inputs to provide an overall assessment of the input plaque images [2]. In particular, in the plaque analysis,

the main problem is the necessity to recognize the contour and the data collection is a crucial phase. Three types of methods may be used to obtain the contour are: a) manual methods; b) interactive methods assisted by the computer; c) automatic methods. Manual segmentation is laborious and increases inter-observer and intra-observer variability [1]. Several algorithms for the segmentation of carotid arteries have been proposed in Ultrasound (US) imaging. In the study of Loizou [3, 4], various snake segmentation methods, with initialization based on the blood flow image, were tested in the context of 2-D longitudinal images of carotid plaques. The plaque was segmented in 2-D longitudinal images [5, 6, 7] by using a combination of gradient-based segmentation, that is a snake segmentation method, and a fuzzy K-means algorithm with an initialization based on pixel echogenicity. In Golemati et al. [8], Hough transforms were used to perform the segmentation of 2-D longitudinal and cross-sectional images of plaques. Recently, Computer Aided Diagnosis (CAD) systems have been developed to improve the capability of clinician to interpret medical images and to differentiate between benign and malignant tissues [9]. The aim of this study was the evaluation of the ability of US in characterizing plaque morphology and composition compared to the analysis of the same plaque on 3T MR.

Chapter 2

Materials and Methods

This chapter reports the techniques used to segment the plaques carotid. We reported the watershed algorithm used for automatic segmentation.

2.1 Study population

We studied 44 subjects, 22 with and 22 without carotid artery stenosis. All subjects were randomly enrolled. The Watershed algorithm, implemented using MATLAB 7.6, was tested on US images. For all the subjects, the analysis was performed including the anamnestic risk clinical factors (diabetes, smoking, hypertension, dyslipidemia). The patients (mean age 63.82 ± 16.66 years) presented stenosis at common (CCA), internal (ICA) and external (ECA) carotid artery between 20% and 60% with about 35% median and have all risk factors that generate the formation of atherosclerotic plaque. The 22 subjects without stenosis (mean age 57.04 ± 21.04 years) presented very low risk factor levels. Detailed

socio-demographic characteristics are summarized in table 2.1. The subjects were recruited from IRCCS Centro Neurolesi "Bonino-Pulejo" of Messina. Local Ethics Committee approval was obtained and all subjects gave informed consent.

TABLE 2.1: Socio-demographic characteristics.

	Patients
N.	22
Age ($mean \pm SD$)	63.8 ± 16.7
Smoker (%)	27.3
Ex Smoker (%)	31.8
Non Smoker (%)	40.9
Diabetes (%)	22.7
Dyslipidemia (%)	72.7
Hyperintension (%)	59.1

2.2 Ultrasonographic data acquisition

The CCA, ICA and ECA US data were obtained as longitudinal cross-sections using a Philips iU22 ultrasound system (Philips Healthcare, Eindhoven, The Netherlands) with an L9-3 probe and included B-Mode (i.e. greyscale) and Colour Doppler image sequences. The vascular carotid preset on the machine was used (Vasc Car preset, persistence low, XRES and SONOCT on) and the gain was optimized by the operator who is an experienced vascular sonographer. We used 44 Echo ColorDoppler images which were stored in a database to be read by the algorithm automatically and sequentially.

2.3 MRI Protocol

The patients underwent a MRI examination with MRI scanner operating at 3.0 T (Achieva, Philips Healthcare, Best, The Netherlands), by using a 32-channel

SENSE head coil. The MRI protocol included: T1 [TR=8ms, TE=4ms, slice thickness/gap=1/0 mm, number of slices= 173, field of view 240 mm], T2-weighted [TR=3.0s, TE=80ms, slice thickness/gap=3.0/0.3 mm, number of slices= 30, field of view 230 mm], axial fluid-attenuated inversion recovery (FLAIR), as well as magnetic resonance angiography (MRA) examinations that included an intracranial 3D time of flight acquisition and an aortic arch through circle of Willis dynamic [TR=10ms, TE=4ms, slice thickness/gap=1/0 mm, number of slices= 65, field of view 200 mm]. The total examination time was of 21 minutes 26 seconds

2.4 Manual Method

The manual segmentation consisted of manual contour of the carotid plaque. The manual delineations were performed by using a system implemented in Matlab (Math Works, Natick, MA). In our study, after pre-processing phase, the plaque profile on all longitudinal ultrasound images was delineated by a neurovascular expert with more than 3 years of clinical experience and blinded to the presence of plaques. The carotid plaque parameters were extracted and saved for comparison with the automatic segmentation method.

2.5 Automatic Method

The dynamic series were retrospectively transferred as anonymized DICOM (Digital Imaging and Communications in Medicine) files to the CAD system. The algorithm implemented a series of processing steps. After reading the B-mode image, to obtain a better segmentation gradient filter was applied (pre-processing

phase). Watershed technique was used to segment the carotid plaques (processing phase). The B-mode features included average signal echogenicity on plaque region (features extraction phase), including finally, the classification phase of plaques. The analysis of the images was automatically performed without any user interaction.

2.6 Pre-Processing

The segmentation of Echo ColorDoppler images is difficult because of variable imaging parameters, overlapping intensities, noise, gradients, motion, blurred edges, normal anatomical variations artifacts. The ultrasound artifacts can be classified as to their sources which are physiologic (for, e.g., motion, different speeds of sound, and acoustic impedance of tissues), equipment (dimension of the ultrasound beam and the converter array), and technical imaging (mode B, spectral Doppler, and color Doppler ultrasound) [10]. Therefore, before applying any approach to carotid artery stenosis, there are generally two pre-processing steps that have to be carried out: first, the removal of artifacts from images and second, the removal of non-plaque features from the image. We considered 44 images, reporting the results obtained on a single one (fig. 2.1) of a patient affected by a fibrocalcific atherosclerotic plaque of 25-30% grade of stenosis localized in the bifurcation of the common carotid artery. As we wanted to maximize performance of the image segmentation methods, it was necessary to remove image in-homogeneities generated by the bias field and suppress the random noise generated by digital acquisition. This cause difficulties in applying techniques for the recovery of the contour of the object. We have applied a filter for removal of artifacts from images. In particular, we applied Sobel filter to detect edges of image. The Sobel operator calculates the

gradient of the image intensity at each point, giving the direction of the largest possible increase from light to dark and the rate of change in that direction. In (fig. 2.2) we showed the obtained image with filter application.

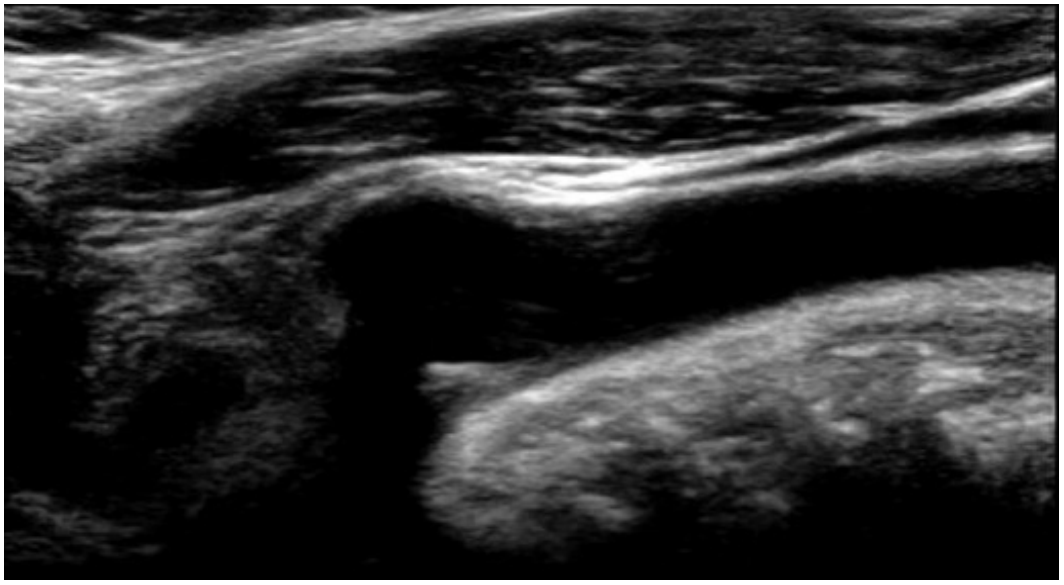

FIGURE 2.1: *US image of a 25-30% grade of stenosis localized in the bifurcation common carotid artery.*

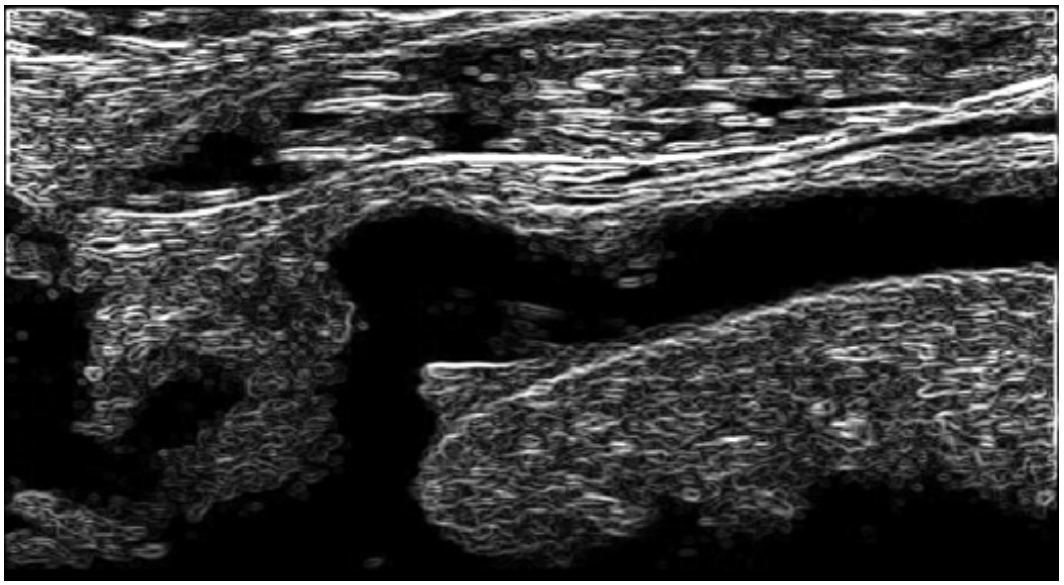

FIGURE 2.2: *Sobel filter image.*

2.7 Processing

To determine foreground objects in the image through Watershed technique, we used the flooding algorithm [11]. Let the original grayscale image be I, the gradient image λ $I$is then computed. Image gradient is analogous to the hills and hollows of a landscape, and the analogy is continued by imagining rain pouring over the landscape, where the water falling on the landscape would flow down to the minimum. Thus, in an immersive simulation of this landscape, water floods from catchment basins when the altitude reaches the local maximum. A dam is therefore built to prevent the basins from merging when two floods originating from different catchment basins meet (fig. 2.3).

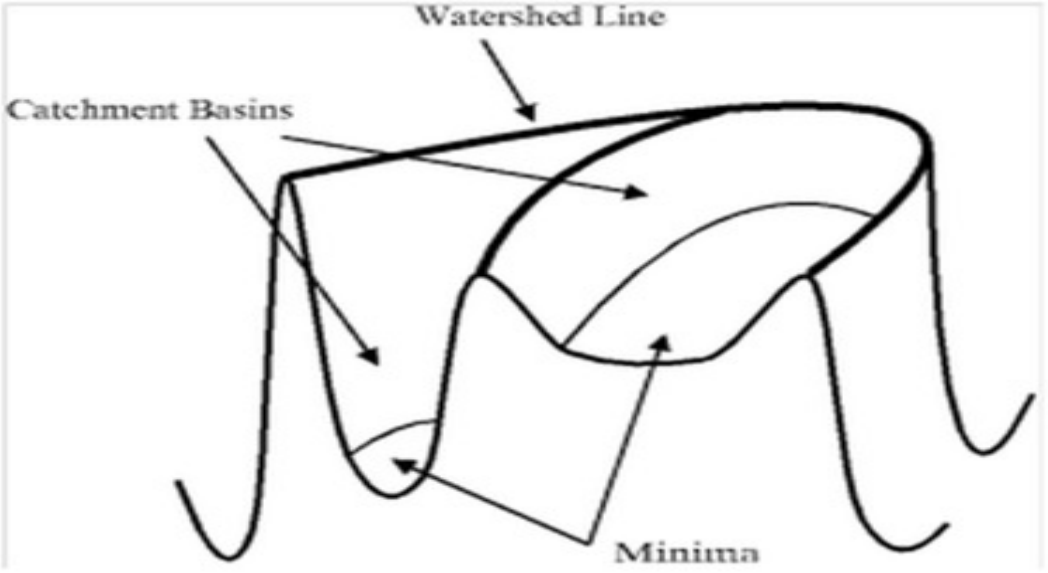

FIGURE 2.3: *Watershed algorithm diagram.*

Direct application of Watershed transformation on the gradient images produce typically severe segmentation of the image, because of numerous minima: those are present in real (gradient) images due to inherent noise. One possibility to get rid of the false regions is the so-called 'marker image' used to mark those regions that require segmentation, although it is generally difficult to obtain relevant markers

automatically without any interaction by the user [12]. A variety of procedures could be applied here to find the foreground markers, which must connected blobs of pixels inside each of the foreground objects. The markers computation was done by using the morphological operations called opening by reconstruction and closing by reconstruction to clean up the image from stem and dark spats and removing the small blemishes without affecting the overall shape of the segmented objects. We used erosion-based gray-scale reconstruction (2.1):

$$\phi_I^{(rec)}(J) = \bigcap_{n \geq 1} \epsilon^n(J) \tag{2.1}$$

where $\epsilon^n(J)$ can be obtained by iterating n elementary geodesic erosion, which is defined as (2.2):

$$\epsilon^{(I)}(J) = (J \ominus b) \cup I \tag{2.2}$$

where b is the flat structuring element of size I and stands for pointwise maximum. Followed by dilation-based gray-scale reconstruction (2.3):

$$\Gamma_I^{(rec)}(J) = \bigcup_{n \geq 1} \delta^n(J) \tag{2.3}$$

where $\delta^n(J)$ can be obtained by iterating an elementary geodesic dilation, which is defined as (2.4):

$$\delta^{(I)}(J) = (J \oplus b) \cap I \tag{2.4}$$

where b is the flat structuring element of size I and $\cap$ stands for pointwise minimum. These techniques are more effective at removing small blemishes without affecting the overall shapes of the objects. The computation of the regional maxima of these reconstructed images is done to get smooth edge foreground objects.

Then, we computed background markers and applied transformed Watershed for segmentation. The obtained image after Watershed segmentation is a color image in which the ROI found are colored. Finally, we superimposed this image (pseudo-color label matrix) on top of the original image (fig. 2.4). Successively, the algorithm applied the Cluster Analysis on some parameters extracted from the plaques.

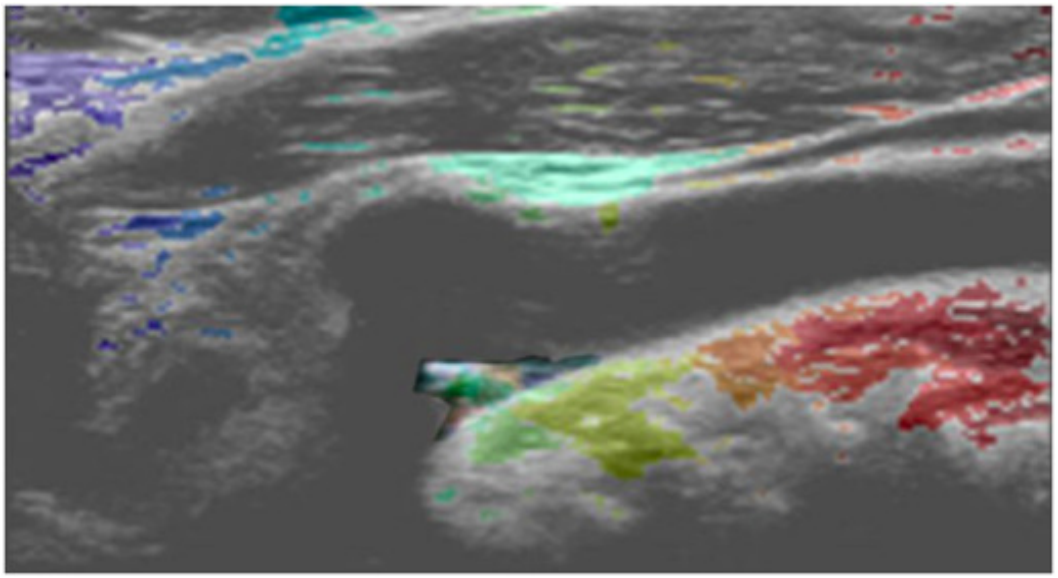

FIGURE 2.4: *Image obtained with Watershed algorithm.*

2.8 Feature Extraction

To describe morphologic characteristics, 12 shape-based and texture feature parameters were calculated. The parameters extracted from each ROI are those that are taken into account also by clinicians to describe the morphology of stenosis: perimeter; area; distance; average signal echogenicity; centroid. For each ROI, we considered the average signal echogenicity feature. This parameter is normally expected to have values between 0 and 1 (non-plaque), (2.5):

$$0 \leq \frac{EchogenicityMean_{singleROI}}{EchogenicityMean_{image}} \leq 1 \tag{2.5}$$

If the output value exceeds 1, the system classified the region as plaques (2.6):

$$\frac{EchogenicityMean_{singleROI}}{EchogenicityMean_{image}} \geq 1 \tag{2.6}$$

The regions that satisfy the condition (2.6) correspond to suspected regions so we built a minimal set of three parameters: average signal echogenicity, distance of image center and centroid. We have calculated the distances between each ROI and the center of the image and we calculated the centroids of each ROI.

2.9 Statistical Analysis

Continuous variables were expressed as $mean \pm standarddeviation$. A parametric analysis was carried out because the results of the Shapiro-Wilk normality test indicated that most of the target variables were normally distributed. Analysis of variance, using Fisher's exact test (F-Test) was used to assess whether a

significant difference existed between data set obtained following different procedures. The F-Test is highly useful when the aim of the study is to evaluate a precision of a measurement technique. In fact, analysis of variance consists of factorization of the total variance into a set of partial variances, which correspond to different and estimated variations. For continuous data, the concordance correlation coefficient (CCC) was used for assessing agreement between 3.0T and US methods. The ICC considers the total variation in measurements across all of the plaques and calculates proportion of the variation that can not be attributed to method differences. The maximum ICC value is 1.00. Overall, ICC values above 0.75 indicate good reliability. Pearson correlation has been used to assess whether there was a relationship between results obtained from automatic and manual segmentation. Analyses were performed using an open source R3.0 software package (http://www.r-project.org). A 95% of confidence level was set with a 5% alpha error. Statistical significance was set at $p < 0.05$.

Chapter 3

Results

This chapter described the results obtained from manual and automatic segmentation. These results show that there no statistically significant difference between the two methodologies.

3.1 Fisher's exact test

The F-Test was then used to verify that the data sets were comparable. For US and MR we obtained no statistically significant difference between the two methodologies (table 3.1). Also, F-test no highlighted significant variance differences between the two methodologies ($p > 0.05$). The values of three plaque parameters obtained by automatic segmentation were highly significantly correlated with those obtained from manual segmentation ($r_1 = 0.78$, $r_2 = 0.84$, $r_3 = 0.89$, with $p < 0.001$).

TABLE 3.1: Parameters obtained from manual and automatic segmentation in US and RM image.

Parameters	**Manual Segmentation**	**Automatic Segmentation**
US Perimeter	66.60 ± 12.75	65.52 ± 11.42
US Area	523.91 ± 16.0	521.88 ± 16.85
US Mean Echogenicity	225.20 ± 15.67	226.12 ± 18.92
MRI Perimeter	67.89 ± 12.76	66.80 ± 12.54
MRI Area	522.91 ± 15.49	522.16 ± 16.10
MRI Mean Echogenicity	227.16 ± 17.14	226.80 ± 17.62

3.2 Concordance Correlation Coefficient

The mean perimeter, area and mean echogenicity obtained by manual segmentation were showed in table 3.1, respectively, while those obtained by automatic segmentation were showed in 3.1. CCC was calculated on three extracted parameters to evaluate the consistency of two methods. The resulting CCCs were significant for all the three parameters (mean echogenicity: $CCC_1 = 0.78(95\%CI : 0.55–0.90)$; perimeter: $CCC_2 = 0.81(95\%CI : 0.61–0.92)$; area: $CCC_3 = 0.89(95\%CI : 0.75–0.95)$. We analyzed also the variability of three parameters by the Bland-Altman Plot (Fig. 3.1).

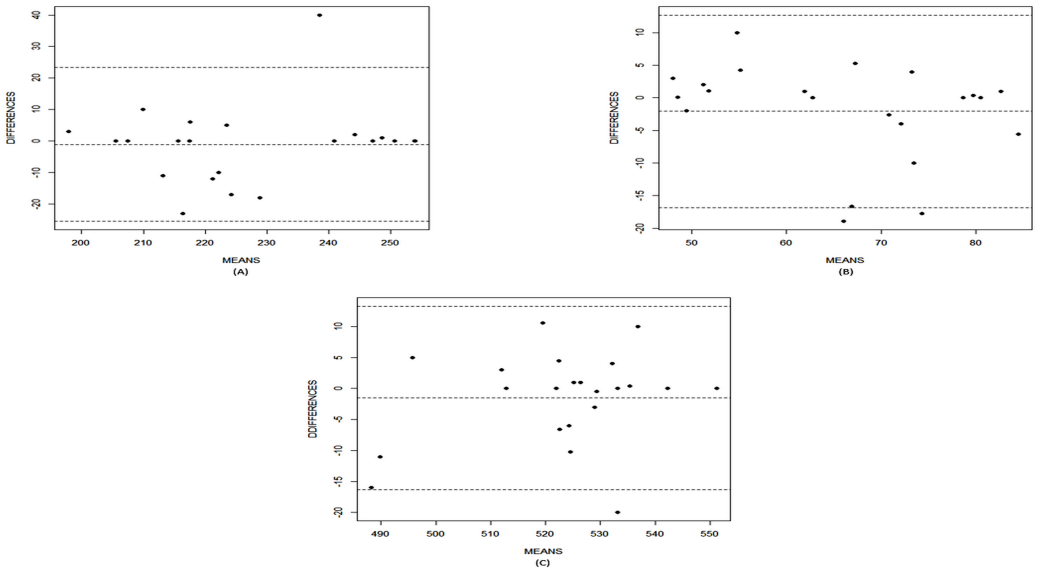

FIGURE 3.1: *Bland-Altman plots for interscan variability of three parameters. A) Mean Echogenicity; B) Perimeter; C) Area.*

Chapter 4

Discussion

Quantitative characterization of atherosclerotic carotid and plaque classification are crucial in the diagnosis and treatment planning. The aim of this study was the evaluation of the ability of US in characterizing plaque morphology and composition compared to the analysis of the same plaque on 3T MR. The algorithm allows to extract information about the descriptive morphology of the ROI: the observation of the value of the average signal echogenicity demonstrates if this feature is typical of the plaque presence or not. In a previous study [9], we have developed a CAD system capable of discriminating the plaque from non-plaque features and also to identify the location and size of each plaque in the US images. In addition, Cluster Analysis was used to solve the problem of undesidered over-segmentation results produced by the Watershed technique and to reduce the number of false detections. From the obtained results by ROC curve we can suppose that our algorithm could be particularly helpful for an objective identification of plaques. By the preliminary experimental results for 44 images, the proposed method can almost find all regions that are plaques, with a diagnostic accuracy of 89%. In fact, we have seen that echogenicity significantly differs between plaques

and non-plaques. To improve specificity without significantly reducing sensitivity, morphologic features have been implemented in clinical routine as further diagnostic criteria in US image. Our algorithm uses the grayscale image converted from the color image. These parameters had a translational impact related to the segmentation of plaques with different characteristics of shape, size and contrast. From ROC curve analysis, we have obtained that if the level of signal average echogenicity is more than 236.8 (cut-off $k = 236.8$) the ROI is considered as a plaque, with a diagnostic accuracy of 89%. CAD systems have been developed to improve the capability of clinician interpretation of medical images and differentiation between benign and malignant tissues [13, 14, 15, 16]. In this study, we have applied the CAD images of US and MRI and compared the results obtained by this automatic method compared to manual segmentation. The efficiency of clinicians' interpretation can be improved in terms of accuracy and consistency in detection/diagnosis, while their productivity can be improved by reducing the time required for reading the images [17]. The computer outputs are derived using various techniques in computer vision to present some of the significant parameters such as the location of suspected lesions and the likelihood of malignancy of detected lesions. Generally, CAD systems are executable on all imaging modalities and all kinds of examinations. Acharya et al. [18] recently presented a CAD system using two different databases consisting of images that characterize the textural differences in these symptomatic and asymptomatic classes using several grayscale features based on a novel combination of trace transform and fuzzy texture. In this case, the accuracy in first database is higher than ours. Seabra et al. [19] developed an ultrasound-based diagnostic measure that quantifies plaque activity (the likelihood of the asymptomatic lesion to produce neurologic symptoms). This information is used to build an enhanced activity index, which considers the

conditional probabilities of each relevant feature belonging to either symptomatic or asymptomatic groups. This measure was evaluated on a longitudinal study of 112 asymptomatic plaques and shows high diagnostic power. Also, in this case the processing step consists of a manual segmentation.

Chapter 5

Conclusions

The automatic plaque segmentation and the developed characterization package could be useful for clinicians to quantify the morphological and texture features and to improve objectivity and efficiency the plaque interpreting. We demonstrated that an automatic image segmentation system can be used to identify, characterize and measure the atherosclerotic plaques in the carotid artery diseas.The watershed algorithm is feasible and has a good agreement with the expert neurologist. Our results showed a very high comparison between US and MRI examinations. From the results obtained, there were no significant differences between the two techniques. The minimal difference is, probably, related to the fact that the US and MRI numerical data were obtained by the operator in a total manual modality.

Bibliography

[1] Zhu X, Zhang P, Shao J, Cheng Y, Zhang Y, Bai J. *A snake-based method for segmentation of intravascular ultrasound images and its in vivo validation.* Ultrasonics 2011;51:181–189.

[2] Kyriacou EC, Pattichis C, Pattichis M, et al. *A review of noninvasive ultrasound image processing methods in the analysis of carotid plaque morphology for the assessment of stroke risk.* IEEE Transactions on information technology in biomedicine 2010;14(4):1027-1038.

[3] Loizou CP, Pattichis CS, Istepanian RSH, Pantziaris M, Nicolaides A. *Atherosclerotic carotid plaque segmentation* . In Proc. 29th Ann. Int. Conf. IEEE Engineering in Medicine and Biology Society (EMBS) , San Francisco, CA, 2004.pp. 1403–1406.

[4] Loizou CP, Pattichis CS, Pantziaris M, Nicolaides A. *An integrated system for the segmentation of atherosclerosis carotid plaque.* IEEE Trans. Inform. Technol. Biomed. 2007;11(6):661–667.

[5] Delsanto S, Molinari F, Liboni W, Giustetto P, Badalamenti S, Suri JS. *User-independent plaque characterization and accurate IMT measurement of carotid artery wall using ultrasound.* In Proc. 28th Ann. Int. Conf. IEEE Engineering in Medicine and Biology Society (EMBS), 2006.pp.404–2407.

[6] Delsanto S, Molinari F, Giustetto P, Liboni W, Badalamenti S, Suri JS. *Characterization of a completely user-independent algorithm for carotid artery segmentation in 2-D ultrasound images*. IEEE Trans. Instr. Meas. 2007;56(4):1265-1274.

[7] Molinari F, Liboni W, Pavanelli E, Giustetto P, Badalamenti S, Suri JS. *Accurate and automatic carotid plaque characterization in contrast enhanced 2-D ultrasound images*. IEEE Engineering in Medicine and Biology Society (EMBS), 2007.pp.335-338.

[8] Golemati SJ, Stoitsis E, Sifakis G, Balkisas T, Nikita KS. *Using the Hough transform to segment ultrasound images of longitudinal and transverse sections of the carotid artery*. Ultrasound Med. Biol. 2007;33(12),1918-1932.

[9] Bonanno L, Marino S, Bramanti P, Sottile F. *Validation of a computer-aided diagnosis system for the automatic identification of carotid atherosclerosis*. Ultrasound Med Biol. 2015;41(2):509-516.

[10] Amir S, Chowdhry BS, Hashmani M, Hasan M. *The Analysis of the Artifacts due to the Simultaneous Use of Two Ultrasound Probes with Different/Similar Operating Frequencies*. Comput Math Methods Med. 2013;2013:890170.

[11] Vincent L, Soille P. *Watersheds in digital spaces: an efficient algorithm based on immersion simulations*. IEEE Trans. Pattern Anal. Mach. Intell. 1991;6:583–598.

[12] Parvati K., Prakasa Rao BS, Mariya Das M. *Image segmentation using gray-scale morphology and marker-controlled Watershed transformation*. Hindawi Publishing Corporation, Discrete Dynamics in Nature and Society, 2008;2008:1–8.

[13] Doi K, MacMahon H, Katsuragawa S, Nishikawa RM, Jiang Y. *Computer-aided diagnosis in radiology potential and pitfalls.* Eur J Radiol 1999;2:97–109.

[14] Giger ML. *Computer-aided diagnosis of breast lesions in medical images.* Comput Sci Eng 2000;2:39-45.

[15] Vyborny CJ, Giger ML, Nishikawa RM. *Computer-aided detection and diagnosis of breast cancer.* Radiol Clin North Am 2000;38: 725-740.

[16] Giger ML, Karssemeijer N. *Computer-aided diagnosis in medical imaging.* IEEE Trans Med Imaging 2001;20:1205-1208.

[17] Doi K. *Computer-aided diagnosis in medical imaging achievements and challenges.* In:World Congress on Medical Physics and Biomedical Engineering. Munich, Germany: 11th International Congress of the IUPESM; 2009.

[18] Acharya UR, Mookiah MR, Vinitha Sree S, Afonso D, Sanches J, Shafique S. *Atherosclerotic plaque tissue characterization in 2-D ultrasound longitudinal carotid scans for automated classification: a paradigm for stroke risk assessment.* Med Biol Eng Comput 2013; 51:513–523.

[19] Seabra J, Pedro ML, Fernandes JF, Sanches J. *Enhanced Activity Index for Predicting Neurologic Symptoms.* Pattern Recognition and Image Analysis Lecture Notes in Computer Science 2011;2011(6669):184–191.
Ultrasound Plaque